ISSN 1067-8212, Russian Journal of Non-Ferrous Metals, 2012, Vol. 53, No. 6, pp. 450–456. © Allerton Press, Inc., 2012.
Original Russian Text © Yu.O. Kucheev, A.B. Straumal, I.V. Mogil'nikova, B.B. Straumal, A.M. Gusak, B. Baretzky, 2012, published in Izvestiya VUZ. Tsvetnaya Metallurgiya, 2012, No. 6, pp. 27–33.

PHYSICAL METALLURGY AND HEAT TREATMENT

Wetting of Grain Boundaries in Hard-Magnetic Nd–Fe–B Alloys

Yu. O. Kucheev[a, b, *], A. B. Straumal[a, b, **], I. V. Mogil'nikova[a, b, *], B. B. Straumal[a, b, ****], A. M. Gusak[c, *****], and B. Baretzky[d, ******]**

[a] *National University of Science and Technology "MISIS", Leninskii pr. 4, Moscow, 119049 Russia*
**e-mail: yuriykuchyeyev@yandex.ru*
***e-mail: Alexander.Straumal@rub.de*
****e-mail: Mogilnikovakira@yandex.ru*
[b] *Institute of Solid-State Physics, Russian Academy of Sciences, Chernogolovka, Moscow oblast, 142432 Russia*
*****e-mail: straumal@mf.mpg.de*
[c] *Department of Theoretical Physics, Cherkasy National University, Shevchenko bul'v. 81, Cherkasy, 18027 Ukraine*
******e-mail: amgusak@ukr.net*
[d] *Karlsruhe Institute for Technology, Institute of Nanotechnologies, Hermann-von-Helmholtz Platz, Eggenstein-Leopoldshafen, 76344 Germany*
*******e-mail: Brigitte.baretzky@kit.edu*

Abstract—Samples of Nd–Fe–B alloys, which have been the main hard-magnetic materials with the highest magnetic energy since the end of the 1980s, are investigated. Magnets based on them are obtained by liquid-phase sintering or spin coating. In this article, wetting of the $Nd_2Fe_{14}B$ grains by the neodymium-enriched liquid phase is investigated. The microstructure of the Fe–12.3 at %Nd–7.6 at %B alloy quenched after annealing at $T = 700$–1100°C in the presence of a neodymium-enriched melt is studied. The acquired data indicate that the transition from incomplete to complete wetting of grain boundaries occurs as the temperature increases. The results are compared with the reference data for alloys of the Nd–Fe–B system obtained by liquid-phase sintering. The relation between the wetting phase transition of grain boundaries and magnetic properties is also discussed.

Keywords: grain boundaries, Nd–Fe–B alloys, hard-magnetic alloys
DOI: 10.3103/S106782121206003X

INTRODUCTION

Two states of a liquid droplet on a solid substrate are possible. If the liquid spreads over the solid surface, this is the situation of complete wetting and contact angle θ between the liquid and the solid phase equals zero. If the liquid droplet forms a finite contact angle, wetting is partial (incomplete). It was shown for the first time by Cahn et al. [1, 2] that the transition (reversible) from partial to complete wetting can occur as the temperature increases and is the surface phase transition.

Currently, there are detailed reviews on wetting phase transitions [3–7]. Later, the Cahn theory was extended to multicomponent systems with critical points (immiscibility regions). Moreover, it can be applied by analogy to wetting phase transitions at grain boundaries (GBs).

The transition from partial to complete wetting is observed for GBs if the grain boundary energy (σ_{GB}) becomes larger than the doubled interphase energy ($2\sigma_{SL}$) solid phase–liquid (Fig. 1). The first reliable results of studying the phase transitions of liquid-phase GB wetting were acquired for two-phase polycrystals in systems Zn–Sn, Zn–Sn–Pb, and Ag–Pb [8, 9]. Later, the Cahn theory on grain-boundary wetting phenomena was applied to a wide circle of experimental data [10]. Subsequently, numerous results also acquired for polycrystalline solids confirmed the existence of GB-wetting phase transitions, particularly for systems Zn–Sn, Al–Cd, Al–In, and Al–Pb ([11] and references therein) and W–Ni, W–Cu, W–Fe, Mo–Ni, Mo–Cu, and Mo–Fe ([12] and references therein).

An exact measurement of the temperature dependence of the contact angle between the GB and liquid and a determination of the temperature of complete wetting (T_w) were performed for individual GBs in specially obtained bicrystals of alloys Cu–In [13], Al–Sn [14], Zn–Sn [15], Al–Zn [16], Sn–Bi [17], In–Sn [18], Zn–Sn, and Zn–In [19]. Moreover, the second wetting phase can be in the solid crystalline state as was shown for alloys Zn–Al [20], Al–Zn [21], Al–Mg [22], and Co–Cu [23], or even in the amorphous state [24–27]. It should be noted that the wetting phase transitions on the surfaces and GBs mainly are first-order transitions (the first derivatives of the surface tension with respect to temperature have discontinuities). However, they can be also of a higher order. In this case, the first derivative of the GB energy (or the surface energy) with respect to temperature changes

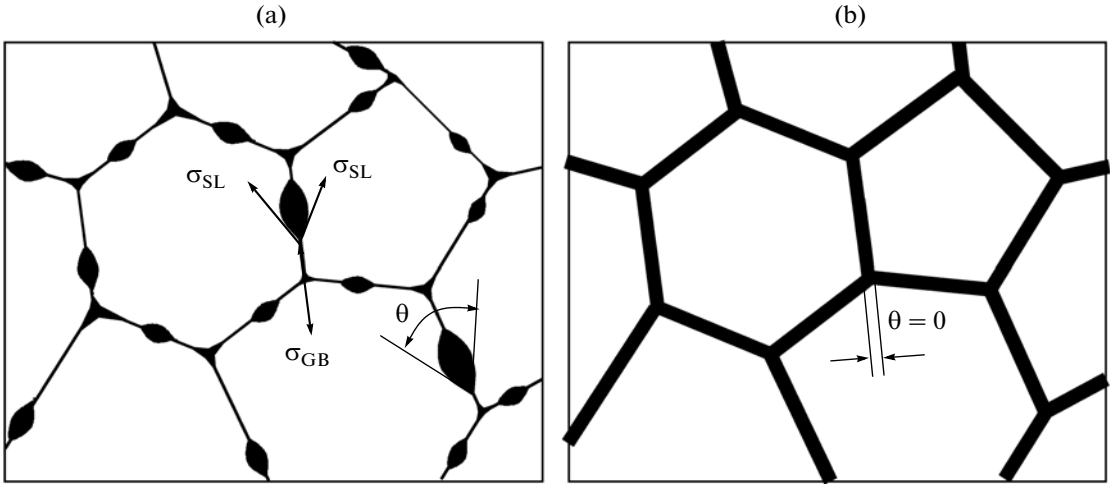

Fig. 1. Schematic image of the polycrystal with grain boundaries wetted (a) partially and (b) completely by the second liquid phase (black). σ_{GB} is the energy of the GB area unit and $2\sigma_{SL}$ is the energy of the area unit of the doubled liquid–solid interface. If $2\sigma_{SL} < \sigma_{GB}$, contact angle $\theta = 0$.

for a finite magnitude by the jump at T_w, while the second derivative with respect to temperature have discontinuity. Continuous wetting phase transitions were predicted in [28, 29] and theoretically studied in detail subsequently [31–33] (see also review [7]).

Experimental evidences on continuous phase transitions were acquired for the first time for liquids only in 1996 [32]. They were later studied for liquid–liquid systems, which were intended for manufacturing oil products containing alkanes in contact with water or aqueous solutions of salts and glucose [33]. A continuous phase transition for the GB was fixed for the first time in the Zn–Al system [16].

The generalized Cahn phase diagram also predicts that the tie line of GB wetting in the two-phase region of the bulk phase diagram can be extended into a single-phase region (the solid solution) as a prewetting line [1]. The surface between the latter and the solidus contains a thin (about several nanometers) layer of a liquid-like phase which is unstable in the bulk. Experimental proof of the existence of prewetting (or premelting) interlayers was also found for metal systems such as Fe–Si–Zn [34–37], Cu–Bi [38–40], Al–Zn [41], and W–Ni [42, 43], as well as for ceramics such as Al_2O_3 [44], Y_2O_3-doped AlN [45], La-doped $SrTiO_3$ [46], Bi_2O_3-doped ZnO [47, 48], and Ca-doped Si_3N_4 [49]. Prewetting was also observed for interphase boundaries [50, 51]. Wetting and prewetting (premelting) phase transitions considerably modify the properties of GBs, particularly diffusion permeability [35–38], mobility [32], plasticity [38, 53, 54], segregation [38–40], and electrical conductivity [55].

Liquid-phase wetting transitions play an important role in processes of the liquid-phase sintering of metals and ceramics [56, 57], in treatment methods of metal–matrix composites in the presence of the melt [58], in heat exchangers based on liquid metals (which are used in nuclear technologies) [59], etc.

The most important alloys of the Nd–Fe–B system, which are obtained by liquid-phase sintering, have been developed actively over the last 25 years due to their excellent magnetic properties [60]. Grains of a ferromagnetic matrix of the $Nd_2Fe_{14}B$ phase in magnets of the Nd–Fe–B system are separated by the intergranular Nd-enriched phase [61]. The degree of separation of the $Nd_2Fe_{14}B$ ferromagnetic grains by such paramagnetic interlayers plays the decisive role in the formation of the magnetic properties of these alloys. Permanent NdFeB magnets are able to conserve a large amount of magnetic energy. Their energy product $(B_dH_d)_{max}$ reaches 512 kJ/m^3, where B_d is the remnant induction (the magnetic induction, which remains in the material after its extraction from the applied external saturation magnetic field) and H_d is the demagnetizing force.

Thus, it is very important to investigate the wetting of the $Nd_2Fe_{14}B$ GBs with a neodymium-enriched liquid phase in detail. The goal of this study was to investigate the classic phase transition in the three-phase region ($Fe_{14}Nd_2B$ (φ phase) + $Nd_2Fe_7B_6$ (η phase) + Nd-enriched liquid phase) of the Nd–Fe–B phase diagram based on the experimental data and to compare these results with the reference data for alloys of the Nd–Fe–B system prepared by liquid-phase sintering.

EXPERIMENTAL

We studied the Fe–12.3 at % Nd–7.6 at % B alloy with a composition close to the most important $Fe_{14}Nd_2B$ magnetic alloy of the Fe–Nd–B system [62, 63]. It was fabricated by vacuum induction melting from high-purity materials (5N Fe, 4N Nd, and

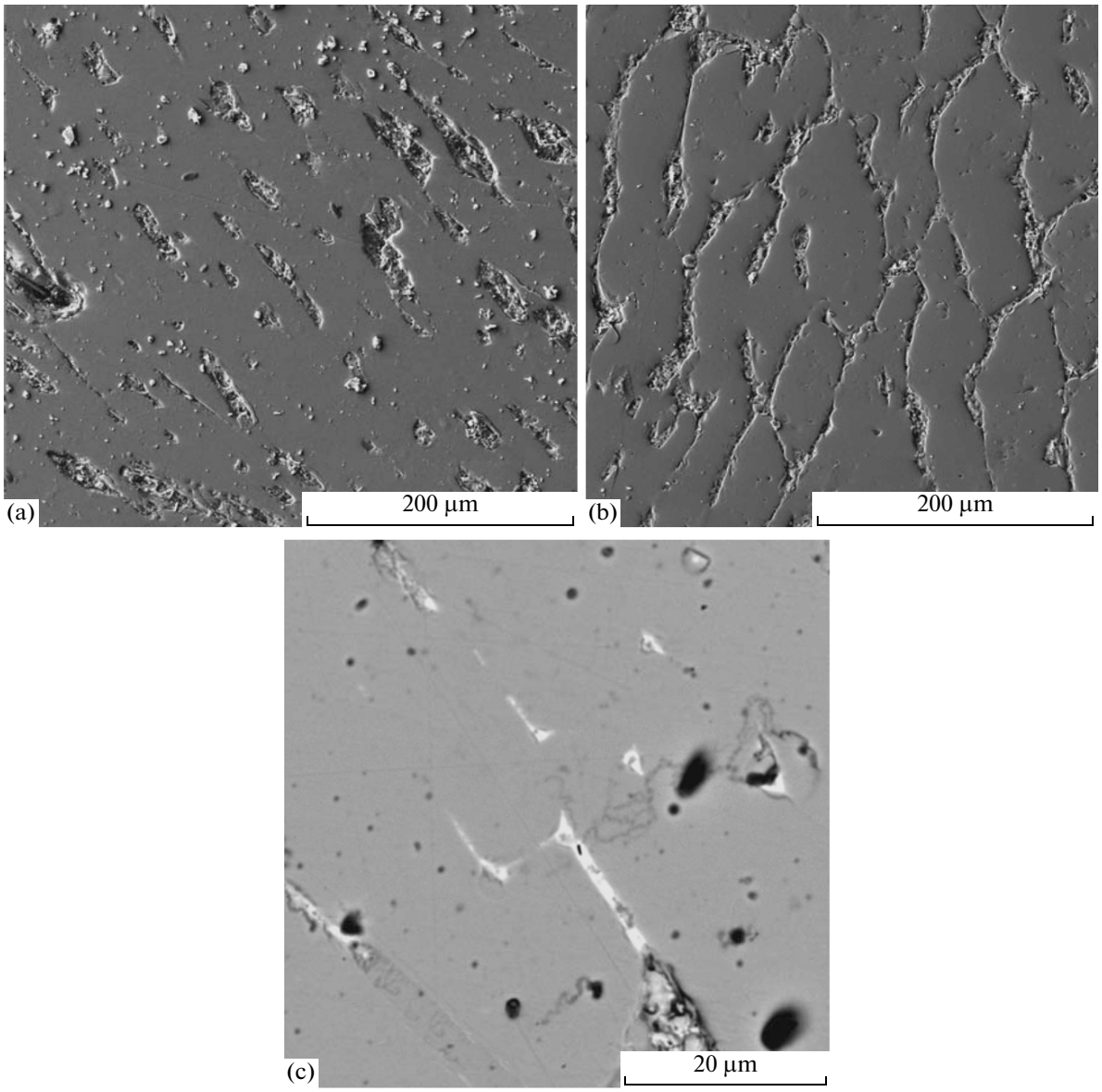

Fig. 2. Micrographs of the Fe–12.3 at %Nd–7.6 at %B alloy. Annealing modes: (a) $T = 900°C$ and $\tau = 2$ h; (b, c) 1000°C and 2 h. Dark gray segments are the grains of the $Fe_{14}Nd_2B$ matrix (φ phase) and light gray segments are the Nd-enriched phase arranged along the boundaries of the $Fe_{14}Nd_2B$ grains. Black inclusions are the pores (the preparation defect of the samples), and white inclusions are the $Nd_2Fe_7B_6$ fine grains (η phase) between the $Fe_{14}Nd_2B$ coarse grains.

4N B). Samples (2 mm thick) were cut from the initial casting (10 mm in diameter) using spark erosion and sealed at room temperature into quartz ampules with a residual pressure of ~4×10^{-4} Pa. Then they were annealed for 2 h at 700, 800, 900, 950, 1000, and 1100°C with accuracy of to ±2°C and quenched into water. The quenched samples were pressed into Technovit® resin and subjected to mechanical treatment, namely, grinding and polishing using diamond paste with abrasive particles (1 μm in size) at the last stage.

After etching, the samples were studied by optical and electron scanning microscopy. We used a Tescan Vega TS5130 MM scanning electron microscope equipped with an INCA Energy 350 energy-dispersive X-ray spectrometer (Oxford Instruments). Optical microscopy was performed using a Neofot-32 microscope equipped with a Canon Digital Rebel XT 10 Mp-camera. A quantitative analysis of the wetting phase transition was performed based on the criteria that the $Fe_{14}Nd_2B$ GB was implied to be wetted completely only if the neodymium-enriched phase interlayer completely covered the GB (Figs. 1b, 2c); if this interlayer was interrupted, we considered the GB as partially wetted (Figs. 1a, 2a, 2b). At least 300 GBs were analyzed for each annealing temperature.

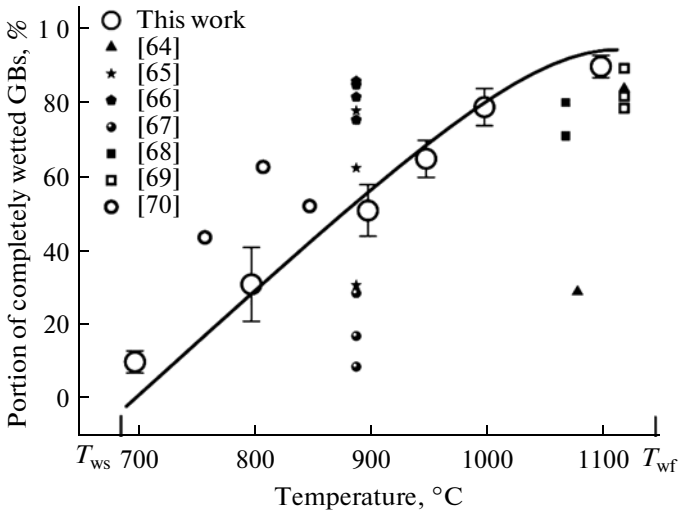

Fig. 3. Temperature dependence of the fraction of the $Fe_{14}Nd_2B$ GBs wetted with the neodymium-enriched phase (the curve and large symbols). The starting and finishing temperatures of the wetting phase transition are $T_{ws} = 690 \pm 10$°C and $T_{wf} = 1150 \pm 10$°C. Small symbols correspond to the results of an analysis of reference data for the samples obtained by liquid-phase sintering.

RESULTS AND DISCUSSION

SEM micrographs for the Fe–12.3 at % Nd–7.6 at % B alloy after annealing at 700 and 1000°C are shown in Fig. 2. Dark gray grains of the $Fe_{14}Nd_2B$ matrix (φ phase) and light gray grains of the Nd-enriched phase, which is arranged at the $Fe_{14}Nd_2B$ GBs, are seen in them. Black regions in the photos are the pores, which are defects of sample preparation, while white segments are the $Nd_2Fe_7B_6$ fine grains (η phase) between the $Fe_{14}Nd_2B$ coarse grains.

Partially and completely wetted GBs of the $Fe_{14}Nd_2B$ phase, as well as the elongated interlayers of the neodymium-enriched phase, are clearly seen in Figs. 2a and 2b. These interlayers form the chains along the partially wetted $Fe_{14}Nd_2B$ GBs. Most of them are completely wetted with the neodymium-enriched phase, which forms continuous interlayers along the GBs separating the $Fe_{14}Nd_2B$ grains from each other.

The Fe–12.3 at % Nd–7.6 at % B alloy in the annealing temperature range under study (700, 800, 900, 950, 1000, and 1100°C) consists of three phases [62, 63]. The main volume is represented by the $Fe_{14}Nd_2B$ grains (φ phase), while the remaining part is the intergranular neodymium-enriched phase, which contains particles of the $Nd_2Fe_7B_6$ solid phase (η phase). These particles are clearly seen in Fig. 2c as small white inclusions.

Figure 3 shows the dependence of the fraction of completely wetted $Fe_{14}Nd_2B$ GBs with the neodymium-enriched phase (large symbols and the line). Only 10% $Fe_{14}Nd_2B$ GBs are completely wetted at 700°C. An extrapolation of the curve of the fraction of wetted boundaries in direction of 0% at low T shows that the temperature of the onset of the wetting phase transition is evaluated as $T_{ws} = 690 \pm 10$°C. About 90% $Fe_{14}Nd_2B$ GBs are completely wetted at $T = 1100$°C. An extrapolation of the curve to the region of 100% gives the finishing temperature of the wetting phase transition $T_{wf} = 1100 \pm 10$°C. Thus, all $Fe_{14}Nd_2B$ GBs are completely wetted with the neodymium-enriched liquid phase above this temperature.

Both partially and completely wetted GBs occur at $T > T_{ws} = 690 \pm 10$°C. It is most probable that this difference in wetting is associated with the spread of the values of specific enthalpy (the energy excess per the area unit) for various $Fe_{14}Nd_2B$ GBs. For example, it was established before that low-energy GBs (for example, twin GBs) can be completely wetted with the second solid phase and contain only chains of solid particles instead of continuous interlayers of this phase [19]. An increase in the fraction of completely wetted GBs with an increase in temperature can be explained by the fact that GBs with various energies also have various temperatures of the wetting phase transition (T_w), for example, GBs with higher energies possesses lower T_w [12, 13].

In addition to our results (large symbols), Fig. 3 also shows data on the investigation of GB-wetting phase transitions based on the published micrographs of NdFeB alloys in publications (small symbols). For this analysis we used micrographs containing no less than 100 grains.

The main distinction between the reference and experimental results of this study is in the acquisition method and purity of starting materials. Our samples were prepared by quenching semi-liquid alloy produced from high-purity starting materials (Nd, Fe, and B), and their final microstructure consists of coarse grains (up to ~500 μm). To the contrary, the ref-

Composition and annealing temperatures of alloys obtained by liquid-phase sintering selected from references to calculate the fraction of wetted boundaries

Alloy composition	Mode of liquid-phase sintering		Annealing modes				Reference
	T_{ls}, °C	τ, h	T_1, °C	τ_1, h	T_2, °C	τ_2, h	
$Nd_{12.8}Fe_{79.8}B_{7.4}$	1080 1120	11	600	1	–	–	[64]
$Fe_{80.85}(NdDy)_{12.99}B_{5.75}Al_{0.24}Ga_{0.1}Zr_{0.07}$	1105	3	900	2	600	3	[61]
$(Pr, Nd)_{14.8}Fe_{78.7}B_{6.5} + Al_{100-x}Cu_x$ (x = 15, 35, 45)	1100	2	890	3	480	2	[65]
$Fe_{68.43}Nd_{28.2}Dy_{2.0}Al_{0.1}Nb_{0.2}Ga_{0.11}B_{0.96}$ + 0, 0.2, 0.3 or 0.5 wt % $Cu_{60}Zn_{40}$	1090	2	890	2	500	3	[66]
$Fe_{78.7}(Pr, Nd)_{14.8}B_{6.5}Fe_{78.7}(Pr, Nd)_{14.8}B_{6.5}$ + 0.6 wt % $Al_{85}Cu_{15}$	1090	2	890	2	550	3	[67]
$Fe_{71}Nd_{22}B_7$ + 0.4 at % MgO or ZnO	1040–1100	2	900	2	600	2	[68]
$Fe_{66.35}Nd_{29.5}Dy_{2.0}B_{1.1}Al_{0.25}Gd_{0.8}$ + 0, 0.1, 0.2 or 0.4 wt % MgO	1120	2.5	510	3	–	–	[69]
$Fe_{78}Nd_{15}Dy_{1.2}Al_{0.8}B_6$	760 810 850	10 min	1000	2	–	–	[70]
	P = 40 MPa						

Note: Subscript in compounds is presented in at %.

erence data are referred to the samples prepared by the liquid-phase sintering of powders at temperature T_{ls}. Moreover, they additionally contain doping components (table) and have a fine-grain structure (of about several micrometers). After sintering, these alloys were annealed from 0.5 to 3 h at one or two temperatures below T_{ls} in several cases (table). It follows from Fig. 3 that the fraction of completely wetted $Fe_{14}Nd_2B$ GBs for the results of an analysis of reference sources is in most cases lower than for our samples.

It is well known that, in order to obtain NdFeB alloys with high magnetic properties, it is necessary for the $Fe_{14}Nd_2B$ grains to be thoroughly separated from each other by a nonferromagnetic phase. It is clearly seen in Fig. 2c that the $Nd_2Fe_7B_6$ particles form "bridges" in some regions, thereby connecting the $Fe_{14}Nd_2B$ grains through the interphase liquid layer of the neodymium-enriched phase. According to the published data, the η phase is ferromagnetic [71], and its presence can ruinously affect the magnetic properties. Therefore, when producing the FeNdB-based permanent magnets, it is desirable to exclude such ferromagnetic overlaps in paramagnetic intergranular layers.

On the other hand, in order to obtain magnetic separation by nonmagnetic interlayers, the thickness of the latter should be on the order of the width of the Bloch walls between the magnetic domains (of about 5 nm) [72]. We can assume that the separation of the $Fe_{14}Nd_2B$ magnetic grains can be attained not only with the help of wetting of the bulk phase by layers having a macroscopic thickness (from several micrometers to 100 nm), but also with relatively thin layers by means of the prewetting–premelting effect [34–51]. The occurrence of several-nanometer-thick layers was fixed several times in the NdFeB alloys [73–75]. However, exact thermodynamic parameters for their formation are still unknown, but theoretical investigations are being continued.

It was proven experimentally that the additional annealing of the samples obtained by liquid-phase sintering at temperatures somewhat lower than eutectic temperature T_{e2} = 665°C [62] increases the coercive force of the material [61, 64–70], which can be associated with the improvement of separation of the $Fe_{14}Nd_2B$ magnetic grains. However, the liquid phase is absent in the FeNdB alloys below temperature T_{e2}, which means that the $Fe_{14}Nd_2B$ GBs should be wetted with the second solid phase.

To produce constant magnets of the NdFeB system, cooling from the liquid phase is used in addition to liquid-phase sintering [76]. Thus obtained amorphous or amorphous-nanocrystalline ribbons are pressed using a binder, after which they are thermally treated in order to obtain the optimal structure and magnetic properties. Severe plastic deformation also makes it possible to obtain a mixture of the amorphous and nanocrystalline phases in the NdFeB alloys [77, 78]. When analyzing the microstructure, it is established that the residual amorphous phase sepa-

rates the $Fe_{14}Nd_2B$ grains even after prolonged annealing. It is probable that wetting of the $Fe_{14}Nd_2B$ GBs by it is similar to that observed for ferromagnetic nanostructured ZnO ribbons in this case [23, 24, 27].

CONCLUSIONS

(i) The neodymium-enriched phase can completely or partially wet the $Fe_{14}Nd_2B$ GBs in the three-phase region ($Fe_{14}Nd_2B$ (φ phase) + $Nd_2Fe_7B_6$ (η phase) + the Nd-enriched liquid phase) of the Nd–Fe–B phase diagram.

(ii) The fraction of completely wetted $Fe_{14}Nd_2B$ GBs increases from 10% (at $T = 700°C$) to almost 100% (at 1100°C). The residual temperatures at which the wetting phase transition starts and finishes are $T_{ws} = 690 \pm 10°C$ and $T_{wf} = 1150 \pm 10°C$, respectively.

(iii) The neodymium-enriched phase between the $Fe_{14}Nd_2B$ grains and at triple junctions contains finely dispersed inclusions of the ferromagnetic η phase ($Nd_2Fe_7B_6$). They can form ferromagnetic "bridges" between the $Fe_{14}Nd_2B$ grains being arranged in intergranular interlayers of the neodymium-enriched phase, which ruinously affects the magnetic properties. Therefore, they should be excluded from produced FeNdB-based constant magnets.

ACKNOWLEDGMENTS

This study was supported by the Allianz Industrie Forschung (project FE.5150.0028.4067); by Max-Planck Institut für Intelligente Systeme (Stuttgart); by the Program of Development of the National University of Science and Technology "MISiS"; by the Russian Foundation for Basis Research, project nos. 10-02-00086, 11-03-00029, and 11-08-90439); and by the Ukrainian Fundamental Research State Fund.

REFERENCES

1. Cahn, J.W., *J. Chem. Phys.*, 1977, vol. 66, p. 3667.
2. Ebner, C. and Saam, W.F., *Phys. Rev. Lett.*, 1977, vol. 38, p. 1486.
3. de Gennes, P.G., *Rev. Mod. Phys.*, 1985, vol. 57, p. 827.
4. Sullivan, D.E. and Telo da Gama, M.M., in *Fluid Interfacial Phenomena*, Croxton, C.A., Ed., New York: Wiley, 1986, p. 45.
5. Dietrich, S., in *Phase Transitions and Critical Phenomena*, Domb, C., Lebowitz, J.L., Eds., London: Academic, 1988.
6. Schick, M., Liquids at Interfaces, *Proc. Les Houches Session XLVIII, 1988*; Charvolin, J., Joanny, J.-F., and Zinn-Justin, J. Eds., Amsterdam: Elsevier, 1990, p. 416.
7. Bonn, D. and Ross, D., *Rep. Prog. Phys.*, 2001, vol. 64, p. 1085.
8. Passerone, A., Eustathopoulos, N., and Desré, P., *J. Less-Common Met.*, 1977, vol. 52, p. 37.
9. Passerone, A., Sangiorgi, R., and Eustathopoulos, N., *Scripta Metall.*, 1982, vol. 16, p. 547.
10. Rabkin, E.I., Shvindlerman, L.S., and Straumal, B.B., *Int. J. Mod. Phys. A*, 1991, vol. 5, p. 2989.
11. Eustathopoulos, N., *Int. Metal Rev.*, 1983, vol. 28, p. 189.
12. Straumal, B.B., *Fazovye perekhody na granitsakh zeren* (Phase Transitions at Grain Boundaries), Moscow: Nauka, 2003.
13. Straumal, B., Muschik, T., Gust, W., and Predel, B., *Acta Metall. Mater.*, 1992, vol. 40, p. 939.
14. Straumal, B., Molodov, D., and Gust, W., *Interface Sci.*, 1995, vol. 3, p. 127.
15. Straumal, B., Gust, W., and Watanabe, T., *Mater. Sci. Forum*, 1999, vol. 294–296, p. 411.
16. Straumal, B.B., Gornakova, A.S., Kogtenkova, O.A., et al., *Phys. Rev. B,* vol. 78, p. 54202.
17. Yeh, C.-H., Chang, L.-S., and Straumal, B.B., *J. Mater. Sci.*, 2011, vol. 46, p. 1557.
18. Yeh, C.-H., Chang, L.-S., and Straumal, B.B., *Mater. Trans.,* 2010, vol. 51, p. 1677.
19. Gornakova, A.S., Straumal, B.B., Tsurekawa, S., et al., *Rev. Adv. Mater. Sci,* 2009, vol. 21, p. 18.
20. López, G.A., Mittemeijer, E.J., and Straumal, B.B., *Acta Mater.*, 2004, vol. 52, p. 4537.
21. Protasova, S.G., Kogtenkova, O.A., Straumal, B.B., et al., *J. Mater. Sci.*, 2011, vol. 46, p. 4349.
22. Straumal, B.B., Baretzky, B., Kogtenkova, O.A., et al., *J. Mater. Sci.*, 2010, vol. 45, p. 2057.
23. Straumal, B.B., Kogtenkova, O.A., Straumal, A.B., et al., *J. Mater. Sci.*, 2010, vol. 45, p. 4271.
24. Straumal, B.B., Protasova, S.G., Mazilkin, A.A., et al., *J. Appl. Phys.*, 2010, vol. 108, p. 73923.
25. Straumal, B.B., Myatiev, A.A., Straumal, P.B., et al., *JETP Lett.*, 2010, vol. 92, p. 396.
26. Mazilkin, A.A., Abrosimova, G.E., Protasova, S.G., et al., *J. Mater. Sci.*, 2011, vol. 46, p. 4336.
27. Straumal, B.B., Mazilkin, A.A., Protasova, S.G., et al., *Thin Solid Films*, 2011, vol. 519, p. 1192.
28. Dietrich, S. and Schick, M., *Phys. Rev. B*, 1985, vol. 31, p. 4718.
29. Shenoy, V.B. and Saam, W.F., *Phys. Rev. Lett.*, 1995, vol. 75, p. 4086.
30. Dietrich, S. and Napiorkowski, M., *Phys. Rev. A*, 1991, vol. 43, p. 1861.
31. Boulter, C.J. and Clarysse, F., *Phys. Rev. E*, 1999, vol. 60, p. R2472.
32. Ragil, K., Meunier, J., Broseta, D., et al., *Phys. Rev. Lett.*, 1996, vol. 77, p. 1532.
33. Ross, D., Bonn, D., and Meunier, J., *Nature*, 1999, vol. 400, p. 737.
34. Semenov, V.N., Straumal, B.B., Glebovsky, V.G., and Gust, W., *J. Cryst. Growth*, 1995, vol. 151, p. 180.
35. Rabkin, E.I., Semenov, V.N., Shvindlerman, L.S., and Straumal, B.B., *Acta Metall. Mater.*, 1991, vol. 39, p. 627.

36. Noskovich, O.I., Rabkin, E.I., Semenov, V.N., et al., *Acta Metall. Mater.*, 1991, vol., 39, p. 3091.
37. Straumal, B.B., Noskovich, O.I., Semenov, V.N., et al., *Acta Metall. Mater.,* 1992, vol. 40, p. 795.
38. Chang, L.-S., Rabkin, E., Straumal, B.B., et al., *Acta Mater.*, 1999, vol. 47, p. 4041.
39. Chang, L.-S., Rabkin, E., Straumal, B.B., et al., *Defect Diffus. Forum*, 1998, vol. 156, p. 135.
40. Schölhammer, J., Baretzky, B., Gust, W., et al., *Interface Sci.*, 2001, vol. 9, p. 43.
41. Straumal, B.B., Mazilkin, A.A., Kogtenkova, O.A., et al., *Phil. Mag. Lett.,* 2007, vol. 87, p. 423.
42. Gupta, V.K., Yoon, D.H., Meyer, H.M., and Luo, J., *Acta Mater.*, 2007, vol. 55, p. 3131.
43. Luo, J., Gupta, V.K., Yoon, D.H., and Meyer, H.M., *Appl. Phys. Lett.*, 2005, vol. 87, p. 231902.
44. Luo, J., Dillon, S.J., and Harmer, M.P., *Microscopy Today*, 2009, vol. 17, p. 22.
45. Pezzotti, G., Nakahira, A., and Tajika, M., *J. Eur. Ceram. Soc.*, 2000, vol. 20, p. 1319.
46. Furukawa, Y., Sakurai, O., Shinozaki, K., and Mizutani, N., *J. Ceram. Soc. Jpn.*, 1996, vol. 104, p. 900.
47. Elfwing, M., Osterlund, R., and Olsson, E., *J. Am. Ceram. Soc.*, 2000, vol. 83, p. 2311.
48. Wang, H. and Chiang, Y.-M., *J. Amer. Ceram. Soc.*, 1998, vol. 81, p. 89.
49. Tanaka, I., Kleebe, H.J., Cinibuluk, M.K., et al., *J. Amer. Ceram. Soc.*, 1994, vol. 77, p. 911.
50. Baram, M. and Kaplan, W.D., *J. Mater. Sci.,* 2006, vol. 41, p. 7775.
51. Levi, G. and Kaplan, W.D., *J. Mater. Sci.*, 2006, vol. 41, p. 817.
52. Molodov, D.A., Czubayko, U., Gottstein, G., et al., *Phil. Mag. Lett.*, 1995, vol. 72, p. 361.
53. Valiev, R.Z., Murashkin, M.Y., Kilmametov, A., et al., *J. Mater. Sci.*, 2010, vol. 45, p. 4718.
54. Chinh, N.Q., Csanádi, T., Győri, T., et al., *Mater. Sci. Eng. A*, 2012, vol. 543, pp. 117–120.
55. Straumal, B.B., Sluchanko, N.E., and Gust, W., *Defect Diffus. Forum*, 2001, vol. 188–190, p. 185.
56. Islam, S.H., Qu, X., and He, X., *Powder Metall.*, 2007, vol. 50, p. 11.
57. Wei, D.Q., Meng, Q.C., and Jia, D.C., *Ceramic Int.,* 2007, vol. 33, p. 221.
58. Solek, K.P., Kuziak, R.M., and Karbowniczek, M., *Arch. Metall. Mater.*, 2007, vol. 52, p. 25.
59. Shatilla, Y.A. and Loewen, E.P., *Nuclear Technol.*, 2005, vol. 151, p. 239.
60. Sagawa, M., Fujimura, S., Togawa, N., et al., *J. Appl. Phys.*, 1984, vol. 55, p. 2083.
61. Yu, L.Q., Zhong, X.L., Zhang, Y.P., et al., *J. Magn. Magn. Mater.*, 2011, vol. 323, p. 1152.
62. Matsuura, Y., Hirosawa, Y., Yamamoto, H., et al., *Jap. J. Appl. Phys. Pt, 2-Lett.*, 1985, vol. 24, p. L635.
63. Schneider, G., Henig, E.-T., Petzow, G., and Stadelmaier, H.H., *Zt. Metallkunde,* 1986, vol. 77, p. 755.
64. Madaah Hosseini, H.R. and Kianvash, A., *J. Magn. Magn. Mater.*, 2004, vol. 281, p. 92.
65. Yan, M., Ni, J., Ma, T., et al., *Mater. Chem. Phys.*, 2011, vol. 126, p. 195.
66. Wu, Y., Ni, J., Ma, T., and Yan, M., *Physica B*, 2010, vol. 405, p. 3303.
67. Ni, J.J., Ma, T.Y., Cui, X.G., et al., *J. Alloys Compd.*, 2010, vol. 502, p. 346.
68. Mo, W., Zhang, L., Liu, Q., et al., *J. Rare Earths*, 2008, vol. 26, p. 268.
69. Yu, L.Q., Zhang, J., Hu, S.Q., et al., *J. Magn. Magn. Mater.*, 2008, vol. 320, p. 1427.
70. Mo, W., Zhang, L., Shan, A., et al., *Intermetal*, 2007, vol. 15, p. 1483.
71. Fidler, J., *IEEE Trans. Magn.,* 1985, vol. 21, p. 1955.
72. Kronmüller, H., *Handbook of Magnetism and Advanced Magnetic Materials*, Chichester: Wiley, 2007.
73. Komuro, M., Satsu, Y., and Suzuki, H., *Mater. Sci. Forum*, 2010, vol. 638–642, p. 1357.
74. Sepehri-Amin, H., Li, W.F., Ohkubo, T., et al., *Acta Mater.*, 2010, vol. 58, p. 1309.
75. Zern, A., Seeger, M., Bauer, J., and Kronmüller, H., *J. Magn. Magn. Mater.*, 1998, vol. 184, p. 89.
76. Li, S., Gu, B., Tian, H., et al., *J. Appl. Phys.*, 2002, vol. 19, p. 7514.
77. Stolyarov, V.V., Gunderov, D.V., Popov, A.G., et al., *J. Magn. Magn. Mater.*, 2002, vol. 242–245, p. 1399.
78. Stolyarov, V.V., Gunderov, D.V., Valiev, R.Z., et al., *J. Magn. Magn. Mater.*, 1999, vol. 196–197, p. 166.